

Technical Report for the Office of Naval Research

Title:

“Development of an acetate-fed or sugar-fed microbial power generator for military bases”

PI: Bruce E. Rittmann, Arizona State University

Award #: N00014-10-M-0231

Report period: 9/1/2010 – 1/1/2011

20110125491



DEFENSE TECHNICAL INFORMATION CENTER

Information for the Defense Community

DTIC® has determined on 1/26/11 that this Technical Document has the Distribution Statement checked below. The current distribution for this document can be found in the DTIC® Technical Report Database.

DISTRIBUTION STATEMENT A. Approved for public release; distribution is unlimited.

© COPYRIGHTED. U.S. Government or Federal Rights License. All other rights and uses except those permitted by copyright law are reserved by the copyright owner.

DISTRIBUTION STATEMENT B. Distribution authorized to U.S. Government agencies only (fill in reason) (date of determination). Other requests for this document shall be referred to (insert controlling DoD office).

DISTRIBUTION STATEMENT C. Distribution authorized to U.S. Government Agencies and their contractors (fill in reason) (date determination). Other requests for this document shall be referred to (insert controlling DoD office).

DISTRIBUTION STATEMENT D. Distribution authorized to the Department of Defense and U.S. DoD contractors only (fill in reason) (date of determination). Other requests shall be referred to (insert controlling DoD office).

DISTRIBUTION STATEMENT E. Distribution authorized to DoD Components only (fill in reason) (date of determination). Other requests shall be referred to (insert controlling DoD office).

DISTRIBUTION STATEMENT F. Further dissemination only as directed by (insert controlling DoD office) (date of determination) or higher DoD authority.

Distribution Statement F is also used when a document does not contain a distribution statement and no distribution statement can be determined.

DISTRIBUTION STATEMENT X. Distribution authorized to U.S. Government Agencies and private individuals or enterprises eligible to obtain export-controlled technical data in accordance with DoDD 5230.25; (date of determination). DoD Controlling Office is (insert controlling DoD office).

Objectives of the Project

Our main goal is to develop and optimize a microbial fuel cell (MFC) that uses a non-flammable and renewable fuel, such as acetate or sucrose, to be used in future military missions. Thus, we must design an MFC capable of producing high power densities with minimal potential losses. These characteristics would allow the MFC to be feasible and efficient. Our proposed approach is to optimize each component of MFCs and then use these components in novel reactor designs that yield high power densities.

We have recently finished the first quarter of the project and are beginning the second one. The goals for the first quarter included: (1) testing anode and anion exchange membrane (AEM) materials, (2) developing a mixed culture for sucrose consumption in an MFC, and (3) completing the design of the MFC modules. The goals for the ongoing second quarter include: (1) optimizing the anode medium for anode-respiring bacteria (ARB) using the PCBIOFILM model and short-term experiments and (2) constructing the MFC modules.

We successfully achieved the 3 goals for the first quarter. We tested graphite and stainless steel as anode materials for ARB growth, showing the greater suitability of carbon fibers as anode material (Figures 1-2). We also tested different commercially available AEMs to select for the most suitable for our MFC modules (Figure 3 and Table 1). Using these selected materials, we are underway of constructing our first MFC module (Figure 5).

We also used an enriched consortium of homo-acetogenic bacteria to consume sucrose and convert it into volatile fatty acids (VFAs) that are easily consumed by ARB (Figure 4). This culture produces mainly lactate and acetate as fermentation products and is ready for test in the MFC modules.

1. Anode materials

We compared the performances of acetate-fed microbial electrolysis cells (MECs) with graphite rods and stainless steel meshes as anodes to select the optimum material for use in MFC modules to be tested in the future. We selected meshes made from 316-grade stainless steel for these initial studies. We conducted several trials with the MECs, and the performance of one set of MECs is reported in Figure 1. As expected with graphite rod anodes, we were able to achieve current densities of $\sim 11 \text{ A m}_{\text{an}}^{-2}$ at a poised potential of $-0.4 \text{ V vs. Ag/AgCl}$ (Figure 1a) when starting with anaerobic digested sludge as inoculum. This is consistent with our previous results using graphite as anode material, wherein we have been able to enrich for *Geobacter* spp. and obtain similar current densities at this poised potential (Torres et al., 2009). We were unable to enrich for efficient ARB from an anaerobic digested sludge inoculum using MECs with a stainless steel mesh anode at a poised potential of $-0.4 \text{ V vs. Ag/AgCl}$ (data not shown). When we used enriched ARB cultures as inoculum in stainless steel anode MECs, we observed current generation, but the best current densities were an order of magnitude lower than for graphite rod MECs (Figure 1b).

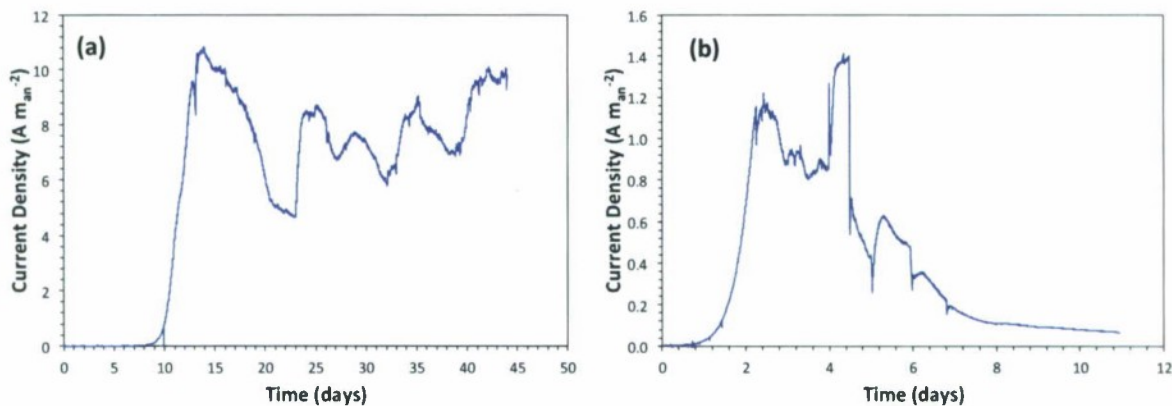


Figure 1. Performance of acetate-fed MECs with (a) a graphite rod anode and (b) a stainless steel anode. The anode potential was poised at -0.4 V vs. Ag/AgCl. The graphite rod anode MEC was operated in batch more until day 22 and then continuously fed for the rest of the duration. The MEC with the stainless steel anode was operated in batch mode through the reported duration of operation.

We postulated that the stainless steel surface hindered the enrichment for ARB efficient in extracellular electron transport (EET) using a conductive biofilm matrix. We thus conducted cyclic voltammetry (CV) scans on one set of graphite rod and stainless steel mesh anode MECs to compare the possible EET mechanisms between the two. These CV scans are shown in Figure 2. The curve for the graphite rod anode MEC (Figure 2a) fits the Nernst-Monod model (Marcus et al., 2007). This successful model fit, in combination with the high current densities, confirms the use of a conductive biofilm matrix for EET. The E_{KA} value determined from the curve fitting (fitting not shown) was -0.43 V vs. Ag/AgCl; this is consistent with values determined for *Geobacter* spp. (Torres et al., 2008).

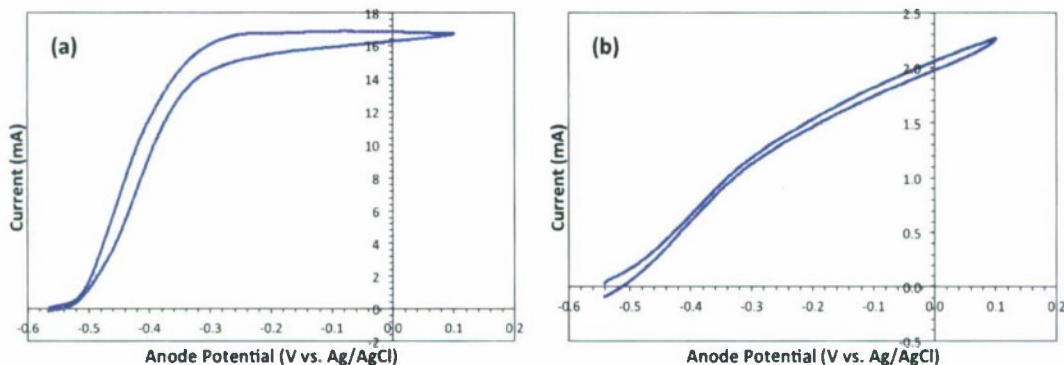


Figure 2. CV scans of acetate-fed MECs with (a) graphite rod anode and (b) stainless steel anode, performed after pseudo steady state. The scan rate was 10 mV s^{-1} .

Contrastingly, even when using an enriched inoculum, the curve for the MEC with the stainless steel mesh anode (Figure 2b) does not fit the Nernst-Monod model. We believe that stainless steel may have induced a change in the EET mechanism due to its inherent properties. We are interested in continuing to evaluate the performance of stainless steel anodes to gain further insight into the reasons for the poorer performance of ARB. However, given the short timeline

of the project, we will move forward with the use of graphite fibers as anodes for the MFC modules we will incorporate these into the MFC modules to be constructed in the coming months.

2. Anion exchange membranes

We selected four anion exchange membranes (AEMs) with a wide range of thicknesses and pH tolerances for the initial characterization studies. The four AEMs selected are listed on Table 1. We used an electrochemical cell with Pt-coated carbon-cloth anode and cathode separated by the AEM for the characterization experiments. We performed electrochemical impedance spectroscopy (EIS) on the electrochemical cell to measure and compare the Ohmic resistance resulting from ion transport between anode and cathode (across the AEM). We determined this resistance for the different AEMs in different liquid electrolytes. Shown in Figure 3 is a sample Nyquist plot generated from EIS analysis. The x-intercept corresponds to the overall solution resistance, which is composed of resistances from the liquid and the solid (AEM) electrolytes. When we compare different AEMs, the contribution from the liquid electrolyte should be the same; thus, any change in overall resistance should be from a difference in AEM resistance.

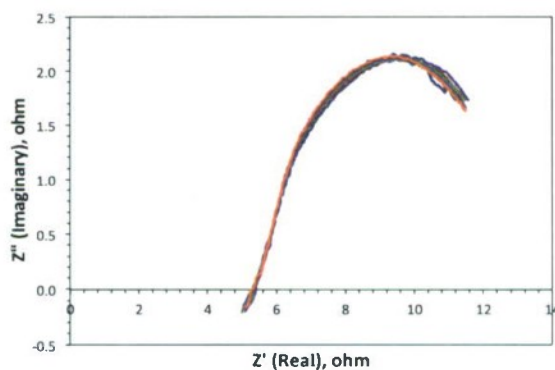


Figure 3. Sample Nyquist plot for Excellion I-200 membrane with 500 mM NaCl.

Table 1 shows a comparison of the various AEMs we tested in terms of their thickness, pH tolerance, and overall solution resistances determined from EIS analysis. The resistances correspond directly with the membrane thickness. The AMI-7001 membrane, which is a standard AEM used by most researchers, is the thickest and, thus, also provides the highest resistance. The Excellion I-200 membrane had a significantly lower resistance compared to AMI-7001 in 100 mM NaHCO₃. Our previous results show that ARB are able to produce higher current densities at higher bicarbonate concentrations (Marcus et al., 2010); 100 mM NaHCO₃ is close to the conditions we will use in the MFC modules. Thus, we operated acetate-fed MECs with this AEM to test its performance under real operating conditions. We were able to achieve similar current densities as MECs with AMI-7001, while observing a decrease in applied voltage. This confirms the lower resistance of Excellion I-200 compared to AMI-7001. However, the Excellion I-200 membrane was compromised in just over a month of operation. We believe this could be due poorer pH tolerance in comparison to the other membrane. Further studies using CO₂ at the cathode to maintain a lower pH could enhance the stability of the Excellion I-200 over long operational periods. However, our preliminary test suggests that this membrane might not be suitable for the MFC modules, even though it provides the least ionic

resistance. We also have concluded that testing the membranes over long-term periods is essential before the final construction of the MFC modules. We recently obtained one additional AEM (Tokuyama Corp.), which we will be testing shortly in real operating conditions. This AEM has significantly lower resistance, and a wide range of pH tolerance.

Table 1. Comparison of the four AEMs characterized for overall solution resistance

Membrane	Thickness (mm)	pH tolerance	Overall solution resistance (ohm)		
			500 mM NaCl	25 mM NaHCO ₃	100 mM NaHCO ₃
AMI-7001 ¹	0.50-0.51	1-10	6.17 ± 0.03	7.17 ± 0.05	7.04 ± 0.05
Excellion I-200 ²	0.32-0.34	NR ⁴	5.32 ± 0.04	7.18 ± 0.05	5.13 ± 0.02
Fumasep FAA ³	0.13-0.15	6-13	3.69 ± 0.03	6.48 ± 0.04	5.90 ± 0.01
Fumasep FAB ³	0.10-0.13	0-13	4.32 ± 0.03	6.15 ± 0.05	5.04 ± 0.02

¹Membranes International, Inc., USA; ²SnowPure, LLC, USA; ³FuMa-Tech GmbH, Germany; ⁴Not reported

3. Development of mixed cultures for sucrose consumption

One of our goals is to develop mixed microbial cultures to convert sucrose to a mixture of VFAs that are readily consumed by ARB to produce high current densities at a high Coulombic efficiency (the fraction of electrons from the electron donor that ends up as electric current). To achieve this, we follow a two-step strategy. Sucrose conversion to the desired VFAs is carried out first by an enriched culture. The second step involves ARB that are acclimatized to efficiently consume the VFAs from the first step.

We set up a 0.5-L batch reactor fed with homo-acetogenic enrichment media of the following composition (in 1 L): KH₂PO₄ – 0.2 g; NaCl – 1 g; NH₄Cl – 0.5 g; KCl – 0.1 g; MgCl₂ · 6H₂O – 0.25 g; CaCl₂ · 2H₂O – 0.175 g; BES – 6.02 g (for selective methanogenic inhibition), NaHCO₃ – 4.2 g; trace mineral media as published in Parameswaran et al (2009) – 1mL; ATCC vitamins solution – 0.5 mL, Fe²⁺ at 4 g/L – 1 mL; and Na₂S · 7H₂O – 0.1 mL. We added 10 mmoles of sucrose to the batch reactor. The initial medium pH was stable at around 6.75. We had previously enriched a consortium of homo-acetogenic bacteria from the suspension of an H-type MEC that produced current from a syntrophic interaction between homo-acetogens and ARB (Parameswaran et al, 2011). We added 5 mL of the enrichment culture to serve as inoculum for the batch electron balance study (1% of reactor volume).

Batch reactions proceeded immediately, leading to complete sucrose utilization by the second day (Figure 4). The reactor pH dropped to 6.05 on day 2, but quickly stabilized back to 6.5 after that time point, and it remained stable until the end of batch operation (day 7). The electron balance ranged from 52% (day 7) to 90% (day 4) of the total electrons input to the system. Of the characterized soluble products at the end of the batch run, lactate was the dominant sink, followed by acetate. Formate is a precursor for homo-acetogenesis, is considered an intermediate for acetate synthesis (Ha et al, 2008), and should be considered as a readily utilized substrate when homo-acetogenesis is not limiting. Lactate, acetate, and formate constitute about 40% of the total electrons from sucrose at the end of the batch test.

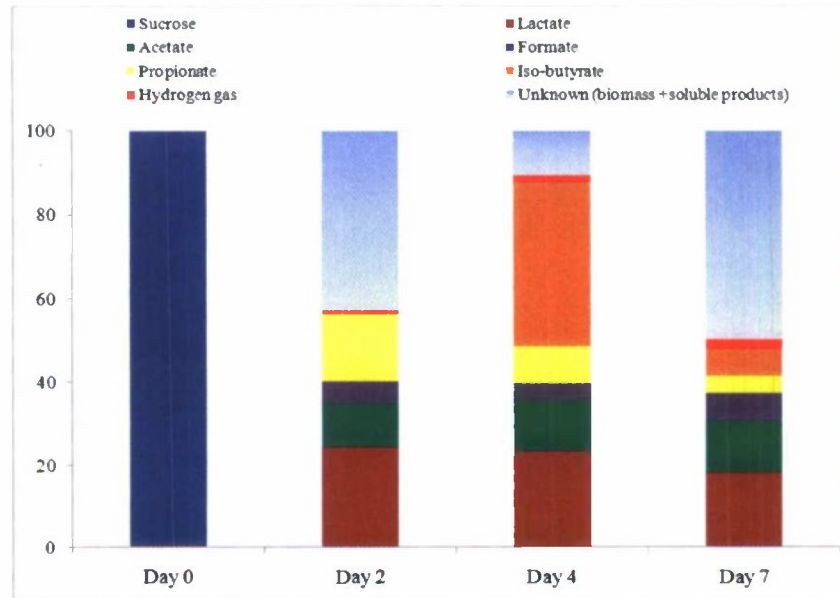
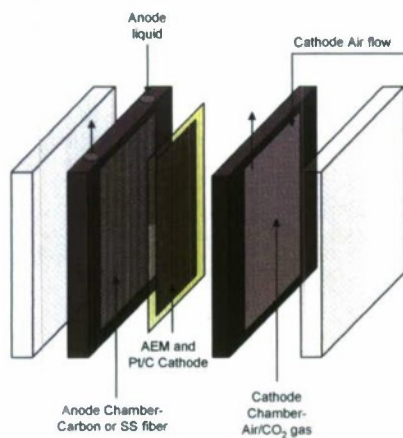


Figure 4. Electron distributions in a batch reactor fed with sucrose (20 mM) as a function of time. Samples for soluble products were taken until gas production ceased (day 7).

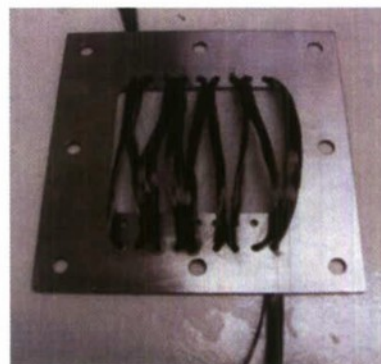
Though the unquantified electrons remain high, we hypothesize that at least 20% of the electrons are in biomass, as observed in homo-acetogenic bacteria that utilize sugars (Drake, 1994). We will evaluate the effect of continuously fed operation on the electron balance. The effluent from the continuous reactor will be fed to an MEC system in which ARB consume the VFAs.

4. Design and construction of microbial fuel cell modules

Based on the materials tested on Sections 1-2, we have started the construction of flat-panel MFCs for both preliminary studies and MFC module operation. Figure 5 shows a schematic and picture of the modules being constructed. The modules will have carbon fibers as anode material with a stainless steel current collector that connects the carbon fibers with the circuit (Figure 5b). For the MFC module, we will use a serpentine flow for air/CO₂, as designed for PEM fuel cells (Figure 5d). This designed will ensure a better availability of O₂ and CO₂ at the cathode surface. We will begin testing the flat panel MFCs shortly.



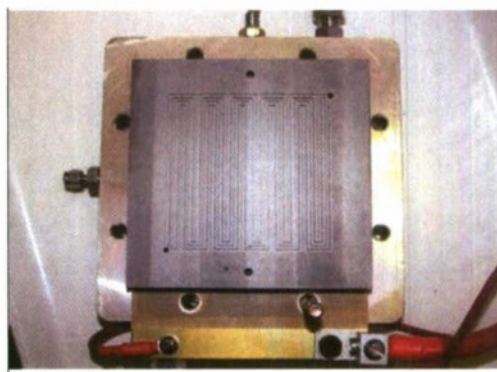
(a)



(b)



(c)



(d)

Figure 5. Schematic (a) and pictures (b-c) of flat panel MFCs. (d) Quad serpentine to be used as air/CO₂ feed to the cathode of flat-panel MFC prototypes.

5. References

- Drake, H.L., 1993. *Acetogenesis*. Chapman & Hall: London.
- Ha, P.T., et al. 2008. Performance and bacterial consortium of microbial fuel cell fed with formate. *Energy & Fuels* 22(1):164-168.
- Marcus AK, Torres CI, Rittmann BE. 2007. Conduction based modeling of the biofilm anode of a microbial fuel cell. *Biotechnol. Bioeng.* 98:1171-1182.
- Marcus AK, Torres CI, and Rittmann BE. 2011. Analysis of a microbial electrochemical cell using the proton condition in the biofilm (PCBIOFILM) model. *Bioresource Technol.* 102(1): 253-262.
- Parameswaran P, Torres CI, Lee HS, Rittmann BE, and Krajmalnik-Brown R. 2011. Hydrogen consumption in microbial electrochemical systems (MXCs): The role of homo-acetogenic bacteria. *Bioresource Technol.* 102(1):263-271.
- Torres CI, Marcus AK, Parameswaran P, and Rittmann BE. 2008. Kinetic experiments for evaluating the Nernst-Monod model for anode-respiring bacteria (ARB) in a biofilm anode. *Environ. Sci. Technol.* 42(17):6593-6597.
- Torres CI, Krajmalnik-Brown R, Parameswaran P, Marcus AK, Wanger G, Gorby YA, and Rittmann BE. 2009. Selecting Anode-Respiring Bacteria Based on Anode Potential: Phylogenetic, Electrochemical, and Microscopic Characterization. *Environ. Sci. Technol.* 43(24):9519-9524.